ORIGINAL PAPER

RJME Romanian Journal of Morphology & Embryology http://www.rjme.ro/

Histological findings for the absorption of small and large liposomes – the basis of future drug delivery and contrast media systems

ROXANA FLORENTINA ŞUFARU[1,2], CRISTINEL IONEL STAN[2], CĂTĂLINA ANIŞOARA PEPTU[3], LIVIU CIPRIAN GAVRIL[2], DRAGOŞ ANDREI CHIRAN[2], DRAGOŞ VALENTIN CRAUCIUC[2], EDUARD GABRIEL CRAUCIUC[4,5], MIHAELA ADELA IANCU[6], RUXANDRA VATAVU[1,2], CODRIN GABRIEL LUCASIEVICI[1,2], ANA MARIA DUMITRESCU[1,2], ANCA SAVA[2,7]

[1] *PhD Student, Doctoral School, Grigore T. Popa University of Medicine and Pharmacy, Iaşi, Romania*

[2] *Department of Morpho-Functional Sciences I, Grigore T. Popa University of Medicine and Pharmacy, Iaşi, Romania*

[3] *Department of Natural and Synthetic Polymers, Cristofor Simionescu Faculty of Chemical Engineering and Environmental Protection, Gheorghe Asachi Technical University of Iaşi, Romania*

[4] *Department of Medicine for Mother and Child, Grigore T. Popa University of Medicine and Pharmacy, Iaşi, Romania*

[5] *Elena Doamna Clinical Hospital of Obstetrics and Gynecology, Iaşi, Romania*

[6] *Department of Internal Medicine, Family Medicine and Labor Medicine, Faculty of Medicine, Carol Davila University of Medicine and Pharmacy, Bucharest, Romania*

[7] *Department of Pathology, Prof. Dr. Nicolae Oblu Emergency Clinical Hospital, Iaşi, Romania*

Abstract

Background and Objectives: The purpose of our study was to obtain and characterize carrier systems in different sizes that can affect oral absorption, since the mechanisms of liposome absorption are not yet fully understood. From stomach to the small intestine, liposomes can be gradually destroyed. Understanding the factors that affect oral absorption leads to developing safe and effective nanosystems to improve the oral delivery of therapeutics. *Materials and Methods:* We determined the efficiency of the absorption of small and large liposomes at the level of gingival mucosa, heart, liver, testicles, kidneys, and lungs, using frozen-section fluorescence microscopy, on rat tissues after liposomes administration. A number of 36 male rats were divided in four groups: control groups, A and C, consisted of six rats each and did not receive liposomes; two other groups, B and D, were the experimental ones, and consisted of 12 male rats each. The animals received small liposomes (75–76 nm) and large liposomes (80–87 nm), respectively, administered either by endogastric tube or intraperitoneal injection. After 24 hours, the animals were sacrificed, and we harvested the organs. We performed frozen sections and analyzed them with fluorescence microscopy. *Results:* The frozen sections obtained from all organs revealed a higher absorption level of small liposomes in the testicles, liver, and gum, while the large liposomes had a greater affinity for the liver, with variations dependent on the route of administration. *Conclusions:* Frozen-section fluorescence microscopy is a reliable technique for visualization of liposome absorption. Based on the size of these nanosystems, we revealed significant absorption for small liposomes in testicles, liver, heart, and gum, and for large liposomes mainly in the liver, compared with the control groups. The study advocates for the usage of liposomes for medical purposes, based on their absorption proprieties.

Keywords: liposomes, absorption, drug delivery system, carrier systems.

Introduction

Liposomes administration by oral route has been studied in several animal trials. However, further investigations are needed to transfer these products into everyday clinical practice. The absorption mechanisms of liposomes have not been fully investigated until now, and for this reason they are not fully elucidated. Liposomes travel to the small intestine after being ingested, and during this journey in the gastro-intestinal (GI) tract they are dispersed in a gradual manner. The transported active drugs into the liposomes structure may be released straightway into the GI tract or they can be handed over to secondary carriers, such as mixed mycelia. Following this transfer to the secondary carriers, the drugs will reach the intestinal mucosa to be absorbed [1–5].

Oral administration of liposomes is partially affected by exposure to gastric acid, but there are liposomes that can survive and are able to pass into the small intestine, where they can be subjected to the action of intestinal surfactants and enzymes. Liposomes that have remained active because of physiological mechanisms come into close contact with the intestinal epithelium and then penetrate the intestinal mucosa. Also, at this level, a possibility of destruction of the liposomes can appear, thus affecting the function of the carrier. However, there are also some particles of liposomes which are withstanding the entire digestion mechanisms, and thus they are fully absorbed and transported into the lymph [6–8].

Pancreatic lipases, bile salts and gastric acid are the main factors involved in liposome clearance, causing breakage and/or inactivation of the drugs susceptible to destruction, like peptides and polypeptides. Thus, the efficiency of oral absorption of liposomes is negatively influenced by all these factors [9].

This is an open-access article distributed under the terms of a Creative Commons Attribution-NonCommercial-ShareAlike 4.0 International Public License, which permits unrestricted use, adaptation, distribution and reproduction in any medium, non-commercially, provided the new creations are licensed under identical terms as the original work and the original work is properly cited.

Aim

The purpose of this study was to determine the efficiency of the absorption of liposomes using frozen-section fluorescence microscopy on rat tissues after liposomes administration through the endogastric tube and intraperitoneal (i.p.) injection in male rats.

Materials and Methods

Materials

In our study, we used the following substances: 1,2-Distearoyl-sn-glycero-3-phosphocholine (DSPC, Avanti); Cholesterol (CHOL, Sigma Aldrich); Chloroform (Sigma Aldrich); Methanol (Sigma Aldrich); Rhodamine [RHD, Octadecyl Rhodamine B Chloride (R18), Sigma Aldrich]; Ferric Chloride hexahydrate (Sigma Aldrich); Ammonium Thiocyanate (Sigma Aldrich); Toluidine Blue (Sigma Aldrich); Milli-Q ultrapure distilled water (Merck). The purity of all these substances was of analytical grade, and this is the reason while they were used without supplementary purification.

Preparation of liposomes labeled with Rhodamine

The selected technique used for the preparation of liposome formulations namely small, unilamellar vesicles (SUV) and multilamellar vesicles (MLV) liposomes was the thin film hydration method [10] with minor modifications. At first, DSPC (120 mg) and CHOL (80 mg) were dissolved in a Chloroform/Methanol 1:1 (*v/v*) mixture (4 mL/4 mL). Evaporation (Heidolph Laborota 4002 rotary evaporator – 60 rpm/35°C/reduced pressure) was performed to extract the solvents from a round bottom flask of 100 mL. A thin film on the flask wall was obtained, and afterwards, the formed lipid film was hydrated with 10 mL of RHD solution at 25°C. Next, vortex shaking was used and spontaneous formation of MLV occurred. The MLV labeled RHD suspension was introduced in an ultrasonic bath for 10 minutes, at a temperature of 25°C, to eliminate the aggregates that were previously formed, and to obtain a homogeneous suspension. The separation of MLV from non-absorbed RHD was achieved by water washes *via* centrifugation (12 spins at 15 000 rpm/15 minutes). Further, SUV were obtained from an MLV suspension prepared as mentioned above, which was extruded repeatedly through a polycarbonate membrane of 400 nm, 200 nm, and 100 nm, respectively. An Avanti Polar Lipids mini-extruder (Avanti Polar Lipids, Inc., Alabaster, AL, USA) was used for the latter procedure. Finally, the obtained RHD-labeled SUV suspension was purified by dialysis for five days using Milli-Q water, with a cellulose ester membrane bag (molecular weight cut-off 2400 Da).

Determination of phospholipid concentration by Stewart assay

Ferrothiocyanate has been obtained by solving 27.03 g of Ferric Chloride hexahydrate and 30.04 g of Ammonium Thiocyanate in double-distilled water and volumized it to one liter.

For the phospholipid (PL) quantification, a Stewart assay was utilized [11]. The Stewart assay presents two advantages. PL headgroups with Ammonium Ferrothiocyanate form a chemical complex, which is red in color and can be quantitatively evaluated by means of spectrophotometry, following extraction into an organic solvent, like Chloroform. Another advantage is represented by the fact that the inorganic phosphate does not interfere with the test.

The quantitation of PL from MLV and SUV suspension was spectrophotometrically performed after purification. The following procedure was used: first, an Ammonium Ferrothiocyanate solution (0.1 M) and a specific calibration curve for DSPC were prepared. The PL concentration was determined by mixing 0.5 mL of MLV or SUV suspension with 2 mL Chloroform and 2 mL Ammonium Ferrothiocyanate solution (0.1 M) into 10 mL quoted tubes and covered with aluminum foil in duplicate. Then, each tube was vortexed vigorously for 30 seconds and then placed for 20 minutes into room environment to complete the reaction. After the reaction was completed, the lower layer was removed using a Pasteur pipette. The Chloroform phase containing the PL was spectrophotometrically analyzed at 485 nm. Finally, the PL concentration from MLV and SUV suspension was obtained by comparing the PL content with the standard calibration curve, previously prepared.

The determined PL concentrations *via* Stewart assay were 13 mg/mL (MLV) and 14.5 mg/mL (SUV). After purification, the result that we obtained was 20 mg/mL.

MLV and SUV size determination *via* laser diffractometry

The size of MLV and SUV liposomes was analyzed by laser diffractometry technique (Shimadzu SALD-7001). MLV and SUV (50 µL) suspensions were placed for sonication for 10 minutes in a room environment using an ultrasound sonication bath from Bandelin Sonorex. After this step, the resulting suspension was placed into a 10 mL double distilled water in a quartz cuvette, and then analyzed. The cuvette was fitted with a stirring system to prevent decantation, since we needed to perform all measurements three times to minimize possible errors in the preparation process.

The granulometric distribution of the MLV and SUV curves was determined using laser diffraction (LD) and was characterized by a unimodal aspect and a submicronic range diameter (75–87 nm) (Figures 1 and 2).

Laboratory animals

In the present experiments, 36 white, non-genetically modified, healthy male Wistar rats (3-month-old), 200–250 g of weight, were used. A required Ethics Approval No. 93/14.06.2021 was obtained from Grigore T. Popa University of Medicine and Pharmacy, Iaşi, Romania. The animals were purchased from the Cantacuzino National Medical Military Institute for Research and Development, Bucharest, Romania, and were accommodated within the CEMEX Laboratory (Advanced Center for Research and Development in Experimental Medicine) at the Grigore T. Popa University of Medicine and Pharmacy, Iaşi.

All rats were kept in a standard environment (25°C temperature, 60% humidity) and a balanced diet with appropriate intake of vitamins and minerals was administrated.

At the beginning of the experiment, the weight of rats was measured because the liposomes should be administered as a dose per kg body weight.

We used four groups of rats (Tables 1 and 2). Groups A and C were the control groups, each of them consisting of six adult male rats that did not receive liposomes.

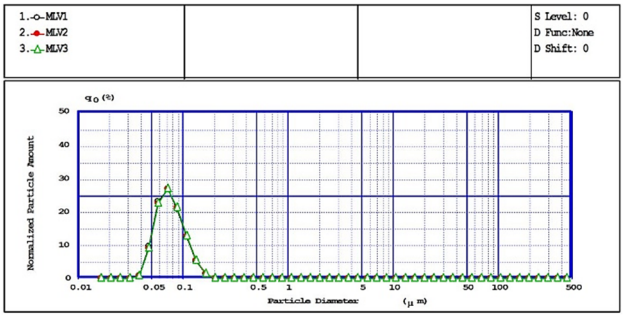

Figure 1 – ***MLV particle size distribution curves obtained by LD. Diameter in nm: MLV1: 75; MLV2: 76; MLV3: 76. LD: Laser diffraction; MLV: Multilamellar vesicles.***

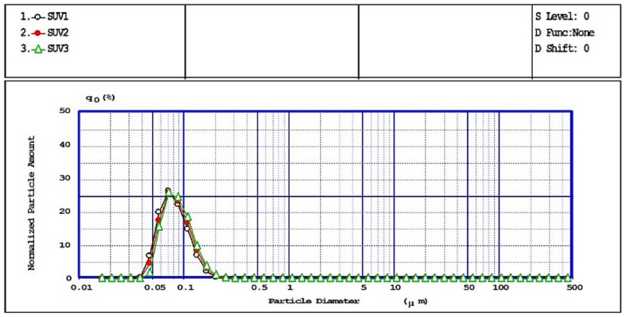

Figure 2 – ***SUV particle size distribution curves obtained by LD. Diameter in nm: SUV1: 80; SUV2: 83; SUV3: 87. LD: Laser diffraction; SUV: Small, unilamellar vesicles.***

Table 1 – ***Administration of small liposomes (75–76 nm) by different routes***

Group	No. of animals	Gender	Administration method	Amount of liposomes [mg/kg body weight]	Administration period [days]
A (control)	6	M	None	n/a	n/a
B (experimental)	6	M	Intraperitoneal	0.2	5
B (experimental)	6	M	Endogastric tube	0.2	5

M: Male; n/a: Not available (applicable).

Table 2 – ***Administration of large liposomes (80–87 nm) by different routes***

Group	No. of animals	Gender	Administration method	Amount of liposomes [mg/kg body weight]	Administration period [days]
C (control)	6	M	None	n/a	n/a
D (experimental)	6	M	Intraperitoneal	0.2	5
D (experimental)	6	M	Endogastric tube	0.2	5

M: Male; n/a: Not available (applicable).

Two other groups, B and D, were the experimental groups and consisted of 12 male rats each. The animals received small liposomes (75–76 nm) and large liposomes (80–87 nm), respectively, that were administered by endogastric tube or by i.p. injection.

The 12 rats of Group B received small liposomes; in half of them, we used the endogastric tube of administration and in the other three, we used i.p. route of administration. The 12 rats of Group D received large liposomes; in half of them, we used the endogastric tube of administration and in the other three, we used i.p. route. Liposomes administration was realized in a single dose (0.2 mg/kg body weight), once a day, for five consecutive days.

After completion of those five days, all animals were sacrificed, and the organs (liver, heart, gingival mucosa, kidney, testicle, and lung) were harvested and placed in paraformaldehyde recipients to be studied by fluorescence microscopy.

To obtain the histological sections for fluorescence microscopy, fragments from harvested organs were sectioned on ice using the Leica CM1860 UV microtome from Sf. Maria Children's Emergency Hospital, Iaşi, Romania.

The steps of sectioning on ice were the following: tissue sampling, fixation, embedding in ice, sectioning, and displaying on aluminum supports. During the first step, we took a tissue fragment from each rat organ (Figure 3, A and B). For the next two steps (fixation and embedding in ice), we have used the same technique as described in a previously published paper (Sufaru *et al.*, 2023), and each organ fragment was placed on a metal support and covered with a fixative, containing a mixture of glycerol and resins that prevents the formation of ice crystals and increases the freezing rate (Figure 3, C and D) [12]. Each tissue fragment was frozen in cryostat at a temperature of -40°C until it became perfectly opaque. Then, we continued with the fourth step, *i.e.*, sectioning, during which we sectioned the frozen tissue block, making 5.0 µm sections at -16°C (Figure 4A). In the last step, we stretched the sections we have obtained on glass slides using the antiroll plate (Figure 4B) [12]. Meyer albumin was used as an adjuvant for this display. Apart from the other organs, on the gingival sections we used Toluidine Blue staining, a basic dye, to highlight its structural elements. All frozen sections were covered with Fluorescence Mounting Medium (Dako) and then cover glasses were placed on. For microscopic examination, we used Nikon Eclipse E600 fluorescence microscope.

During all these activities, we avoided light exposure of both the slides and the sampled organs.

Results

We performed microscopic examination of all frozen sections we obtained, taking into consideration the size of the liposomes we have administered, and also the route of their administration (Table 3).

Regarding the size and the route of administration, fluorescence microscopic examination revealed the yellow-light fluorescence of the RHD reagent in the liver of 20 out of 24 experimental rats, with various levels of absorption (Groups B and D) (Figure 5, A and B; Figure 6) that signaled the presence of liposomes in the Kupffer cells, as we labeled with RHD the liposomes we have used.

Fluorescence microscopic examination of unstained sections from gingival mucosa revealed a green auto-fluorescence at the level of endothelium and internal elastic lamina of arterioles (Figure 7A), but no fluorescence

determined by the presence of liposomes labeled with RHD was identified in five rats from Group B and in four rats from Group D. Fluorescence microscopic examination of frozen sections from gingival mucosa that have been stained with Toluidine Blue revealed a red fluorescence of the background (Figure 7B).

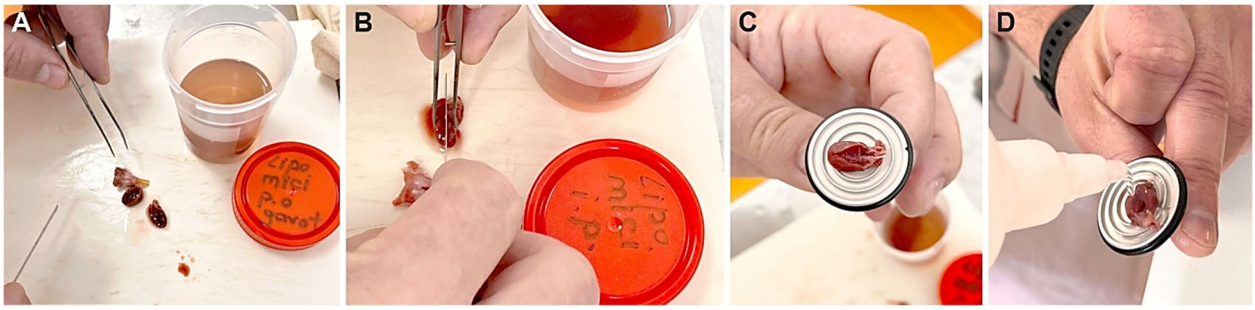

Figure 3 – *(A) Displaying of harvested organs; (B) Sampling of a tissue fragment from each rat organ; (C) Placing the removed organ fragment on the block support; (D) Fixation the organ fragment with freezing fixative.*

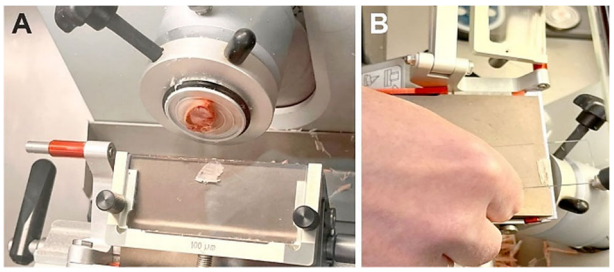

Figure 4 – *(A) Ice sectioning of organ fragment; (B) Display on the slide of the ice section of the organ fragment.*

Table 3 – *Results observed on frozen sections of the harvested organs examined by fluorescence microscopy*

Absorption level based on size of liposomes	Intraperitoneal injection Type of organ						Endogastric tube Type of organ					
	Gum	*Liver*	*Heart*	*Lung*	*Kidney*	*Testicle*	*Gum*	*Liver*	*Heart*	*Lung*	*Kidney*	*Testicle*
Small												
-	1 (16.7%)	1 (16.7%)	3 (50.0%)	3 (50.0%)	4 (66.7%)	1 (16.7%)	4 (66.7%)	2 (33.3%)	3 (50.0%)	3 (50.0%)	4 (66.7%)	4 (66.7%)
+	2 (33.3%)	1 (16.7%)	1 (16.7%)	2 (33.3%)	2 (33.3%)	1 (16.7%)	1 (16.7%)	2 (33.3%)	1 (16.7%)	2 (33.3%)	2 (33.3%)	1 (16.7%)
++	1 (16.7%)	2 (33.3%)	1 (16.7%)	1 (16.7%)		1 (16.7%)	1 (16.7%)	1 (16.7%)	2 (33.3%)	1 (16.7%)		1 (16.7%)
+++	2 (33.3%)	2 (33.3%)	1 (16.7%)			3 (50.0%)		1 (16.7%)				
Large												
-	2 (33.3%)	1 (16.7%)	3 (50.0%)	4 (66.7%)	4 (66.7%)	2 (33.3%)	2 (33.3%)	2 (33.3%)	5 (83.3%)	4 (66.7%)	4 (66.7%)	2 (33.3%)
+	4 (66.7%)	1 (16.7%)	2 (33.3%)	1 (16.7%)	1 (16.7%)	4 (66.7%)	4 (66.7%)	4 (66.7%)	1 (16.7%)	1 (16.7%)	1 (16.7%)	4 (66.7%)
++		3 (50.0%)	1 (16.7%)	1 (16.7%)	1 (16.7%)					1 (16.7%)	1 (16.7%)	
+++		1 (16.7%)										
p-value* (small *vs* large)	0.159	0.910	0.631	0.785	0.422	0.050	0.136	0.327	0.194	0.785	0.422	0.136

*Kruskal–Wallis test.

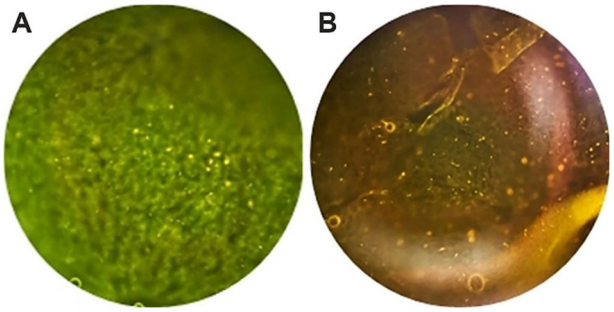

Figure 5 – *Microscopic image of liver tissue displaying small liposomes according to the administration route (×200). Fluorescence of small liposomes administrated by endogastric tube (A) and intraperitoneally (B).*

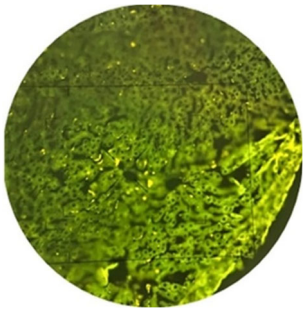

Figure 6 – *Microscopic image of liver tissue displaying fluorescence of large liposomes administered by endogastric tube (×400).*

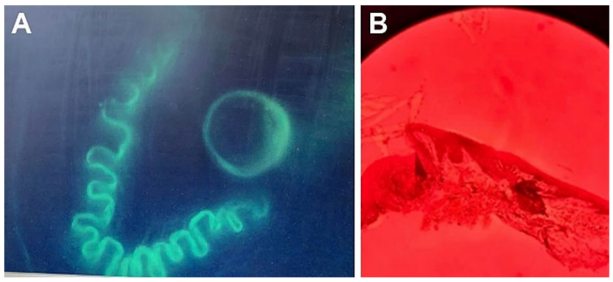

Figure 7 – ***(A) Autofluorescence of internal elastic lamina of arterioles from the gingival chorion following intraperitoneal administration of small liposomes (×400); (B) Absence of fluorescence for large liposomes at gingival level, administered via endogastric tube; Toluidine Blue staining (×100).***

In Group B, in the rats with i.p. administration of small liposomes, the absorption degree of liposomes was higher in testicles (50%), liver (33.3%), and gums (33.3%). The correlation matrix between the degree of absorption of liposomes compared between harvested organs, according to the study group, did not reveal significant differences (p>0.05), except for testicles. In testicles, in Group B, the degree of very high absorption (+++) was found in 50% of subjects, and in Group D, the degree of absorption was only low (+), but was found in most of the subjects, respectively 66.7% (p=0.05). In the rats that received liposomes (small, respectively large) with endogastric tube, the degree of absorption of liposomes did not differ between Groups B and D, in any of the organs (p>0.05) (Table 3).

In the subjects with i.p. administration of small liposomes (Group B), the degree of absorption in the liver was significantly higher compared to the degree of absorption in the gum (p=0.018), heart (p=0.033), and kidney (p=0.025), while in Group D (large liposomes), the degree of absorption in the liver was significantly higher compared to the degree of absorption in the kidney (p=0.050). In the rats administered by endogastric tube, in Group B (small liposomes), significant differences in the degree of absorption were recorded between the gum and testicle (p=0.001), and between liver and testicle (p=0.025), while in Group D (large liposomes), the differences were significant between the gum and testicle (p=0.034), and between the heart and kidney (p=0.040) (Tables 3 and 4).

By plotting the receiver operating characteristic (ROC) curve to highlight the influence of administered liposomes and of the method of administration on the degree of absorbance of the organs examined by fluorescent microscopy, the following aspects are noted (Table 5; Figure 8, A and B):

- in the rats with i.p. administration, the degree of absorption in the liver was noted with a sensitivity (Se) of 83% and a specificity (Sp) of 30% [area under the curve (AUC) 0.712; 95% confidence interval (CI): 0.491–0.934; p=0.085], in the testicles with a Se of 75% and a Sp of 45% (AUC 0.670; 95% CI: 0.448–0.893; p=0.166), and in the heart with a Se of 50% and a Sp of 70% (AUC 0.629; 95% CI: 0.398–860; p=0.295);
- in the rats with endogastric tube administration, the Se/Sp balance of the degree of absorption of the examined organs was not significant (AUC<0.600).

Table 4 – ***Kruskal–Wallis test. Correlation matrix between the degree of absorption of liposomes by type of organ***

Small	Intraperitoneal injection						Endogastric tube					
	Gum	*Liver*	*Heart*	*Lung*	*Kidney*	*Testicle*	*Gum*	*Liver*	*Heart*	*Lung*	*Kidney*	*Testicle*
Gum	–						–					
Liver	0.018	–					0.025	–				
Heart	0.072	0.033	–				0.069	0.091	–			
Lung	0.220	0.436	0.420	–			0.208	0.504	0.221	–		
Kidney	0.360	0.025	0.040	0.729	–		0.301	0.561	0.027	0.729	–	
Testicle	0.003	0.067	0.079	0.268	0.373	–	0.001	0.025	0.069	0.208	0.301	–
Large	**Intraperitoneal injection**						**Endogastric tube**					
	Gum	*Liver*	*Heart*	*Lung*	*Kidney*	*Testicle*	*Gum*	*Liver*	*Heart*	*Lung*	*Kidney*	*Testicle*
Gum	–						–					
Liver	0.318	–					0.108	–				
Heart	0.404	0.404	–				0.106	0.154	–			
Lung	0.360	0.360	0.059	–			0.106	0.154	0.053	–		
Kidney	0.182	0.050	0.040	0.088	–		0.208	0.182	0.040	0.088	–	
Testicle	0.206	0.404	0.270	0.216	0.282	–	0.034	0.102	0.106	0.106	0.208	–

Table 5 – ***Area under the ROC curve***

Test result variable(s)	Area	Standard Error[a]	Asymptotic Significance[b]	Asymptotic 95% CI	
				Lower bound	*Upper bound*
Intraperitoneal injection					
Gum	0.644	0.116	0.242	0.416	0.872
Liver	0.712	0.113	0.085	0.491	0.934
Heart	0.629	0.118	0.295	0.398	0.860
Lung	0.519	0.123	0.878	0.278	0.760
Kidney	0.527	0.123	0.829	0.286	0.767
Testicle	0.670	0.114	0.166	0.448	0.893

Test result variable(s)	Area	Standard Error[a]	Asymptotic Significance[b]	Asymptotic 95% CI	
				Lower bound	*Upper bound*
			Endogastric tube		
Gum	0.356	0.116	0.242	0.128	0.584
Liver	0.288	0.113	0.085	0.066	0.509
Heart	0.371	0.118	0.295	0.140	0.602
Lung	0.481	0.123	0.878	0.240	0.722
Kidney	0.473	0.123	0.829	0.233	0.714
Testicle	0.330	0.114	0.166	0.107	0.552

CI: Confidence interval; ROC: Receiver operating characteristic. The test result variable(s): Gum, Liver, Heart, Lung, Kidney, Testicle has at least one tie between the positive actual state group and the negative actual state group. Statistics may be biased. [a]Under the nonparametric assumption. [b]Null hypothesis: true area = 0.5.

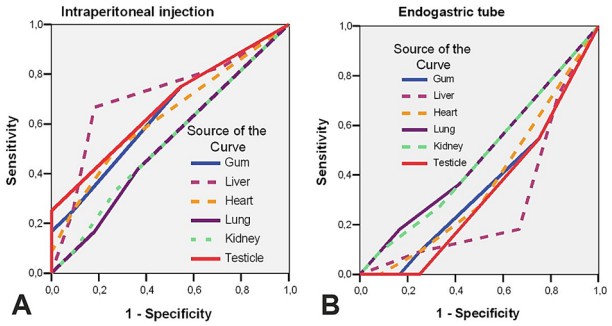

Figure 8 – ***(A and B) ROC curve. Sensitivity and specificity of treatment depending on organs examined by fluorescence microscopy. ROC: Receiver operating characteristic.***

Discussions

Liposomes are lipid-based nanoparticles (NPs) that are widely used as nanomedicines, particularly in cancer therapy, due to their high biosafety. Another important application is represented by their use in contrast media in medical imaging.

Liposomes can be considered as non-biological multi-functional complex drugs, which improve the solubility of drugs, protect them against enzymatic degradation, and provide longer systemic circulation. Because they can be made in different sizes, liposomes can be used for both topical and systemic administration of different drugs. Liposomes are small, artificial vesicles that are formed from PLs and CHOL, and thus have a similar structure to natural plasma membranes. The PLs in their structure are phosphatidylcholine or saturated PLs with long acyl chains and are arranged in a double layer [13].

Because of the double layer, liposomes, like other cells, allow a watery environment inside. The presence of the water-based core allows loading of the lysosomes with both hydrophobic and/or hydrophilic drugs, so these NPs have many therapeutic benefits [14]. To be visualized, liposomes must be labeled with certain substances, such as lipophilic cyanine dyes that fluoresce in visible light. Lipophilic cyanine dyes present high photostability and tight integration in between double-layer structures. They are also hard to change in *in vitro* and *in vivo* environments. After systemic injection, liposomes have a circulatory half-life of 1.3 hours. Fluorescence increases at five minutes after injection, but decreases by 70% at five hours, although it remains above baseline for seven days after injection [15]. In our study, animals were sacrificed 24 hours after the last administration and thus liposomes were still present on sections obtained by ice sectioning.

Previous studies [8] have shown effective accumulation of liposomes in the skin by microscopic studies. Griffin *et al.* demonstrated that systemically injected liposomes bind to capillary endothelium in the skin, and accumulate in dermis and hypodermis, specifically into the extravascular cells. Unexpectedly, shortly after injection, dendritic cells, Langerhans cells or other skin phagocyte subtypes outside the blood vessels internalize liposomes. It is presumed that following the extravasation process, the liposomes lose their polyethylene glycol (PEG) coating and they become more prone to englobing by phagocytes [8].

Our study also demonstrated by microscopic examination that liposomes accumulate in liver Kupffer cells, which also act as macrophages. The identification of liposomes in liver macrophages (Kupffer cells) has shown the systemic biodistribution of small artificial vesicles of liposomes.

Kupffer cells are found in literature also as Kupffer–Browicz cells. They are stellate macrophages located in the sinusoids of the liver and are attached to endothelial cells. The structure and function of Kupffer cells varies with their localization, periportal and centrilobular, respectively. The cells located near portal vein display an increased phagocytic activity supported by a larger diameter and an increased production of lysosomal enzymes. In contrast, the Kupffer cells found in the centrilobular zone produce superoxide radicals in higher quantity [15]. However, their role in rapid clearance of any harmful agent for liver is well established and this fact can explain the presence of liposome inside these cells [16].

Our experimental study proved that small and large liposomes with nanometric dimensions are absorbed and identified at liver, gum, heart, and testicle levels, with variations in absorption dependent on the route of administration. This demonstrates that the usage of liposomes like drug carriers has the advantage of increasing the absorbent effects that are not usually produced without a drug carrier. Thus, liposomes can improve drug loading and drug delivery offering many advantages over traditional dosage forms [17].

The liposomes can also become carrier systems for contrast media administered during medical imaging procedures. One of the challenges in the radiology department is dealing with possible allergies and anaphylaxis to radio-contrast substances. Patients with allergic history or increased reactivity due to immune-related conditions are at a higher risk when injected with contrast media. Moreover, patients

self-declared allergies, to contrast media may deprive them of important imaging investigations [18]. In these situations, pre-procedure testing is paramount, and a solution to decrease the immunogenicity of these substances could offer a safer option to patients with mild to even moderate allergic reactions. Lamichhane *et al.* suggested that if liposomes are conjugating with different labeling probes one can identify the precise localization of these formulations using imaging investigations, *i.e.*, positron emission tomography (PET), single photon emission computed tomography (SPECT), magnetic resonance imaging (MRI). Moreover, the authors emphasis the low-immunogenic proprieties of liposomes, that make these conjugates a contrast media of choice in cases of patients with mild reaction to regular radiocontrast substances [19]. Liposomes encapsulating both Gadolinium contrast medium and thrombolytic medication open perspectives to simultaneously approach specific conditions like stroke, from both an imaging and a therapeutic perspective [20].

We must mention that fluorescence microscopic examination of frozen section from gingival mucosa that have been stained with Toluidine Blue revealed a red fluorescence of the background, as Chelvanayagam & Beazley have shown already in 1997 [21].

On the other hand, fluorescence microscopic examination of unstained sections from gingival mucosa revealed a green fluorescence at the level of endothelium and external elastic lamina. The same aspects have been shown by Li *et al.*, who have demonstrated that there is an autofluorescence signal of arterial blood vessels compared with the venous wall in mice, which originates at the level of elastin fibers [22].

Study limitation

A limitation in our study is represented by the small number of laboratory animals that were approved in the Ethics Approval issued by Grigore T. Popa University of Medicine and Pharmacy, Iași. A greater number of studied rats would have enabled us to perform a statistical analysis with a higher significance of the experimental findings. Moreover, an increased number of microscopically analyzed probes from the harvested organs could have enabled us to propose a more accurate quantification method for the observed liposomes in terms of their concentration in the examined field view.

Conclusions

Frozen-section fluorescence microscopy is a reliable technique for visualization of liposome absorption. Regardless of the size and the route of administration of the liposomes, the fluorescence microscopic examination revealed significant absorption of these nanosystems mainly in the liver and testicles, compared with control groups of animals, moderate absorption in heart and gums, and very low absorption at the level of lungs and kidneys. The study shows that usage of liposomes can bring benefits by implementation in the clinical drug delivery systems and contrast media for specific imaging.

Conflict of interests

The authors declare that they have no conflict of interests.

Institutional Review Board Statement

The animal study protocol was approved by the Ethics Committee of Grigore T. Popa University of Medicine and Pharmacy, Iaşi, Romania (Approval No. 93/14.06.2021).

Funding

This research was funded by Grigore T. Popa University of Medicine and Pharmacy, Iași, Romania, within the research program at the Doctoral School of the first author, R.F.S.

References

[1] Bunker A, Magarkar A, Viitala T. Rational design of liposomal drug delivery systems, a review: combined experimental and computational studies of lipid membranes, liposomes and their PEGylation. Biochim Biophys Acta, 2016, 1858(10):2334–2352. https://doi.org/10.1016/j.bbamem.2016.02.025 PMID: 26915693

[2] Gregoriadis G, Florence AT. Liposomes in drug delivery. Clinical, diagnostic and ophthalmic potential. Drugs, 1993, 45(1):15–28. https://doi.org/10.2165/00003495-199345010-00003 PMID: 7680982

[3] He H, Lu Y, Qi J, Zhu Q, Chen Z, Wu W. Adapting liposomes for oral drug delivery. Acta Pharm Sin B, 2019, 9(1):36–48. https://doi.org/10.1016/j.apsb.2018.06.005 PMID: 30766776 PMCID: PMC6362257

[4] Gregoriadis G. Fate of injected liposomes: observations on entrapped solute retention, vesicle clearance and tissue distribution *in vitro*. In: Gregoriadis G (ed). Liposomes as drug carriers: recent trends and progress. John Wiley and Sons, Chichester, UK, 1988, 3–18. https://worldcat.org/title/573613259

[5] Suk JS, Xu Q, Kim N, Hanes J, Ensign LM. PEGylation as a strategy for improving nanoparticle-based drug and gene delivery. Adv Drug Deliv Rev, 2016, 99(Pt A):28–51. https://doi.org/10.1016/j.addr.2015.09.012 PMID: 26456916 PMCID: PMC4798869

[6] Liu JX, Xin B, Li C, Xie NH, Gong WL, Huang ZL, Zhu MQ. PEGylated perylenemonoimide-dithienylethene for super-resolution imaging of liposomes. ACS Appl Mater Interfaces, 2017, 9(12):10338–10343. https://doi.org/10.1021/acsami.6b15076 PMID: 28281748

[7] Signorell RD, Papachristodoulou A, Xiao J, Arpagaus B, Casalini T, Grandjean J, Thamm J, Steiniger F, Luciani P, Brambilla D, Werner B, Martin E, Weller M, Roth P, Leroux JC. Preparation of PEGylated liposomes incorporating lipophilic Lomeguatrib derivatives for the sensitization of chemo-resistant gliomas. Int J Pharm, 2018, 536(1):388–396. https://doi.org/10.1016/j.ijpharm.2017.11.070 PMID: 29198811

[8] Griffin JI, Wang G, Smith WJ, Vu VP, Scheinman R, Stitch D, Moldovan R, Moghimi SM, Simberg D. Revealing dynamics of accumulation of systemically injected liposomes in the skin by intravital microscopy. ACS Nano, 2017, 11(11):11584–11593. https://doi.org/10.1021/acsnano.7b06524 PMID: 29045127 PMCID: PMC5770233

[9] Tang J, Kuai R, Yuan W, Drake L, Moon JJ, Schwendeman A. Effect of size and pegylation of liposomes and peptide-based synthetic lipoproteins on tumor targeting. Nanomedicine, 2017, 13(6):1869–1878. https://doi.org/10.1016/j.nano.2017.04.009 PMID: 28434931 PMCID: PMC5554706

[10] Moghimi SM, Szebeni J. Stealth liposomes and long circulating nanoparticles: critical issues in pharmacokinetics, opsonization and protein-binding properties. Prog Lipid Res, 2003, 42(6):463–478. https://doi.org/10.1016/s0163-7827(03)00033-x PMID: 14559067

[11] Torchilin VP. Recent advances with liposomes as pharmaceutical carriers. Nat Rev Drug Discov, 2005, 4(2):145–160. https://doi.org/10.1038/nrd1632 PMID: 15688077

[12] Sufaru RF, Radulescu AM, Vatavu R, Sava A, Gavril LC, Popa C. Tissue penetrability as a function of nanoparticle delivery mode. J Med Med Sci, 2023, 14(2):1–4. https://www.interesjournals.org/articles/tissue-penetrability-as-a-function-of-nanoparticle-delivery-mode-95119.html

[13] Powers D, Nosoudi N. Liposomes; from synthesis to targeting macrophages. Biomed Res, 2019, 30(2):288–295. https://doi.

org/10.35841/biomedicalresearch.30-19-058 https://www.alliedacademies.org/articles/liposomes-from-synthesis-to-targeting-macrophages-11299.html
[14] Cauzzo J, Jayakumar N, Ahluwalia BS, Ahmad A, Škalko-Basnet N. Characterization of liposomes using quantitative phase microscopy (QPM). Pharmaceutics, 2021, 13(5):590. https://doi.org/10.3390/pharmaceutics13050590 PMID: 33919040 PMCID: PMC8142990
[15] Basit H, Tan ML, Webster DR. Histology, Kupffer cell. In: StatPearls [Internet]. StatPearls Publishing, Treasure Island, FL, USA, 2023 Jan, 2022 Dec 30. PMID: 29630278
[16] Bilzer M, Roggel F, Gerbes AL. Role of Kupffer cells in host defense and liver disease. Liver Int, 2006, 26(10):1175–1186. https://doi.org/10.1111/j.1478-3231.2006.01342.x PMID: 17105582
[17] Pereira S, Egbu R, Jannati G, Al-Jamal WT. Docetaxel-loaded liposomes: the effect of lipid composition and purification on drug encapsulation and *in vitro* toxicity. Int J Pharm, 2016, 514(1):150–159. https://doi.org/10.1016/j.ijpharm.2016.06.057 PMID: 27863659
[18] Berghi ON, Dumitru M, Vrinceanu D, Cergan R, Jeican II, Giurcaneanu C, Miron A. Current approach to medico-legal aspects of allergic reactions. Rom J Leg Med, 2021, 29(3):328–331. https://doi.org/10.4323/rjlm.2021.328 https://www.rjlm.ro/index.php/arhiv/898
[19] Lamichhane N, Udayakumar TS, D'Souza WD, Simone CB 2nd, Raghavan SR, Polf J, Mahmood J. Liposomes: clinical applications and potential for image-guided drug delivery. Molecules, 2018, 23(2):288. https://doi.org/10.3390/molecules23020288 PMID: 29385755 PMCID: PMC6017282
[20] Šimečková P, Hubatka F, Kotouček J, Turánek Knötigová P, Mašek J, Slavík J, Kováč O, Neča J, Kulich P, Hrebík D, Stráská J, Pěnčíková K, Procházková J, Diviš P, Macaulay S, Mikulík R, Raška M, Machala M, Turánek J. Gadolinium labelled nanoliposomes as the platform for MRI theranostics: *in vitro* safety study in liver cells and macrophages. Sci Rep, 2020, 10(1):4780. https://doi.org/10.1038/s41598-020-60284-z PMID: 32179785 PMCID: PMC7075985
[21] Chelvanayagam DK, Beazley LD. Toluidine blue-O is a Nissl bright-field counterstain for lipophilic fluorescent tracers Di-ASP, DiI and DiO. J Neurosci Methods, 1997, 72(1):49–55. https://doi.org/10.1016/s0165-0270(96)00155-0 PMID: 9128168
[22] Li H, Yan M, Yu J, Xu Q, Xia X, Liao J, Zheng W. *In vivo* identification of arteries and veins using two-photon excitation elastin autofluorescence. J Anat, 2020, 236(1):171–179. https://doi.org/10.1111/joa.13080 PMID: 31468540 PMCID: PMC6904638

Corresponding authors

Liviu Ciprian Gavril, Senior Assistant Professor, MD, PhD, Department of Morpho-Functional Sciences I, Grigore T. Popa University of Medicine and Pharmacy, 16 Universităţii Street, 700115 Iaşi, Romania; Phone +40753–048 788, e-mail: liviu.gavril@umfiasi.ro

Dragoş Andrei Chiran, Senior Assistant Professor, MD, PhD, Department of Morpho-Functional Sciences I, Grigore T. Popa University of Medicine and Pharmacy, 16 Universităţii Street, 700115 Iaşi, Romania; Phone +40740–232 048, e-mail: dragos-andrei.chiran@umfiasi.ro

Received: October 15, 2023

Accepted: December 1, 2023